Plasma-Based Flow Control for Improved Aerodynamic Efficiency

Vishwaijith Lal and Efstratios L. Ntantis[1]

Aerospace Department, Amity University Dubai, Dubai, UAE

Abstract. Plasma flow actuators have emerged as an innovative solution for active flow control, offering unparalleled capabilities to enhance aerodynamic performance. These actuators employ a plasma discharge to generate an electrohydrodynamic (EHD) force, creating ionized regions that interact with airflow to improve boundary-layer stability, delay flow separation, and reduce drag. The plasma actuators consist of two electrodes separated by a dielectric material. A high-voltage AC input is supplied to the electrodes. When the alternating current (AC) amplitude is large enough, the air ionizes in the most significant electric potential region. Ionization forms ions and electrons. The ions move under the drive of an electric field and transfer momentum through collision with neutral gas molecules. In this paper, an experimental study on the laminar and turbulent boundary layers of a low-pressure turbine blade is conducted using dielectric barrier discharge plasma excitation. The results show that the plasma excitation's velocity increase near the wall is significant and long-lived. It can also enhance the performance of traditional control surfaces or the operational flight envelope of air vehicles by providing controls at flight conditions where conventional control surfaces are ineffective.

1 Introduction

Plasma-based flow control leverages the unique properties of plasma actuators to manipulate airflow and improve aerodynamic efficiency. These actuators are compact, surface-mounted devices strategically applied to airfoils, where they operate by generating ionized regions that impart momentum to the surrounding airflow [1]. This technology has effectively addressed critical aerodynamic challenges, including delaying flow separation, suppressing turbulence, and enhancing boundary-layer control. By doing so, plasma actuators significantly boost lift generation and minimize induced drag, offering potential improvements in aircraft performance, energy efficiency, and stability across various operating conditions [2]. Moreover, the versatility of plasma actuators extends their applicability to other domains, including wind turbine efficiency, icing mitigation, and flow control in industrial settings [3]. Plasma actuators come in various types, each suited to specific flow control applications. One of the most common types is the dielectric barrier discharge (DBD), a plasma actuator widely used for aerodynamic applications. It consists of two electrodes separated by a dielectric material. When a high-voltage alternating current (AC) is applied, it generates plasma and produces a body force that manipulates the airflow [4]. It is effective for boundary layer control, separation delay, and noise reduction [5]. Another type is the sliding-discharge plasma actuator, which uses exposed electrodes so the discharge slides along the surface. This configuration enables localized control of flow phenomena, such as vortex generation or suppression [6]. The nanosecond-pulsed plasma (NS-DBD) actuator uses short, high-voltage pulses to produce rapid plasma discharges. This is highly effective for high-speed flow applications, such as shock-wave control in the supersonic and transonic regimes [7]. The Corona discharge actuator uses a single exposed electrode and relies on ionization around it to generate a body force. It is typically used for small-scale flow control due to lower power requirements [8]. The glow discharge plasma actuator generates a continuous plasma layer that can accelerate flow and delay transition. It operates at lower pressures, making it useful for specific aerodynamic or industrial applications [9]. The peristaltic plasma actuator is designed to create periodic plasma discharges. This actuator mimics peristaltic motion and can effectively generate synthetic jets or control flow instabilities [10]. A vectorized plasma actuator uses multiple electrodes to generate directional body forces, enabling more precise control of the flow field. It is often used for applications requiring highly localized adjustments [11]. Each type of plasma actuator has unique advantages and is selected based on specific flow-control requirements, operating conditions, and application area. This study evaluates the impact of plasma excitation on the laminar and turbulent boundary layers of a low-pressure turbine blade, aiming to understand its influence on near-wall velocity profiles and its long-term effectiveness. The broader objective is to assess the feasibility of using plasma actuators to improve the operational efficiency of traditional control surfaces and expand the flight envelope of air vehicles, especially in conditions where conventional control methods are inadequate.

[1] Corresponding author: entantis@amityuniversity.ae

2 DBD Plasma Actuator

DBD plasma actuator consists of two electrodes separated by a dielectric material, as illustrated in Figure 1. Plasma is generated via dielectric barrier discharge in the region between the exposed electrode and the dielectric sheet when a high potential difference is applied across the electrodes. The resulting electric field accelerates the plasma, creating a partially ionized plasma layer near the actuator's surface. The ionization of a molecule (M) in an electric field is shown in Eq.1.

$$\text{Molecule (M)} + \text{Electric Field} \rightarrow M^{+} + e^{-} \quad (1)$$

This acceleration induces a body force interacting with the surrounding neutral air molecules, effectively driving the airflow near the actuator's surface. This mechanism is fundamental to plasma actuators' flow control capabilities. The body force F can be expressed as follows in Eqs 2 and 3, where ρ_e is the charge density, E is the electric field, n is the number density of an ion, and q is the elementary charge of an ion or electron (1.6 x 10^{-19} C), respectively.

$$F = \rho_e \cdot E \quad (2)$$

$$F = q \cdot n \cdot E \quad (3)$$

Due to this potential, plasma actuators have been used to control turbines, wind turbine blades, and holders [12,13]. More recently, they have reduced friction drag by delaying the flow transition [14] or oscillating the flow spanwise [15]. Maintaining sufficient lift in planetary exploration airplanes is a significant development hurdle. For example, in Martian air, the major problem is the gravitational acceleration, which is about 1/3 that of Earth; the atmospheric density is only 1/100, the Reynolds number is 1/100, and the speed is about 2/3 Earth's. The lift coefficient decreases sharply below a Reynolds number of 10 ^5. This explains why active flow control is crucial for operation [16]. This brief review of DBD aerodynamic actuators is not exhaustive. The main goal of this paper is to present the fundamental mechanisms of plasma actuator physics and to demonstrate applications in the active flow control domain.

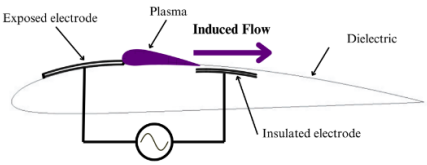

Fig. 1. DBD plasma actuator configuration on Clark Y airfoil

3 DBD Aerodynamic Actuator

A classical setup of the DBD plasma actuator consists of two pairs of dissymmetrical electrodes separated by a dielectric medium, as shown in Figure 1. The airfoil's leading edge will have a positive potential. It will be structured to have a sharp edge facing the adjacent insulated electrode. The insulated electrode would have a greater surface area because it is at a negative potential, which positively affects the velocity of the produced ion flow. When a high voltage (typically 10-50 kV) is applied, a macroscopically uniform surface discharge appears. Still, it is made by microdischarge [17], which occurs at several hundred megahertz (MHz) [18]. An example is illustrated in Figure 2, where the dielectric is Teflon and the applied voltage is 15 kV peak [19].

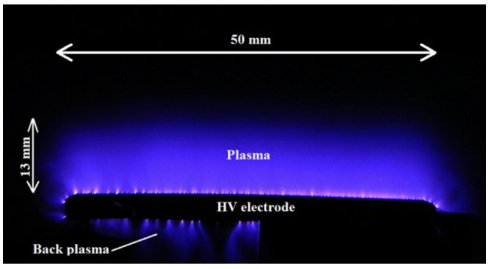

Fig. 2. Top-view image of the plasma [19]

The plasma discharge, combined with the specific electrode configuration, generates a jet along the actuator surface, mimicking the effect of traditional blowing methods [17]. These plasma-induced jets alter the aerodynamic boundary layer, enhancing flow momentum, particularly in the near-wall region above the surface. Over the past decade, numerous

experimental [20-27] and computational [28] studies have examined the fundamental physical mechanisms underlying electrohydrodynamic (EHD) interactions. A velocity profile of the tangential wall jet is depicted in Figure 3 [29].

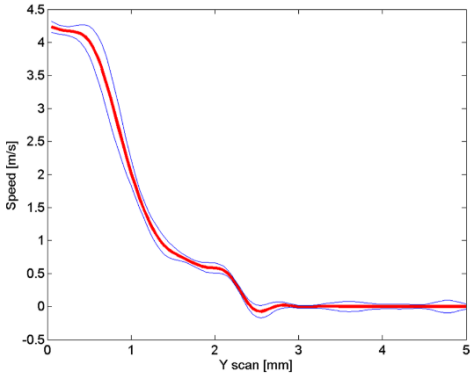

Fig. 3. Standard pitot tube velocity profile for DBD plasma actuator (red line) [29]

The measurement was performed using a glass pilot tube positioned 2 mm downstream of the plasma discharge region and moved parallel to the actuator's surface. Peak velocities were typically observed in the range of 5-6 m/s. When DBD actuators are aligned parallel to the incoming flow, the interaction between the induced and incoming flows generates vortices that propagate downstream. These vortices, known as plasma vortex generators (PVGs), enhance mixing and flow control, as illustrated in Figure 4 [30].

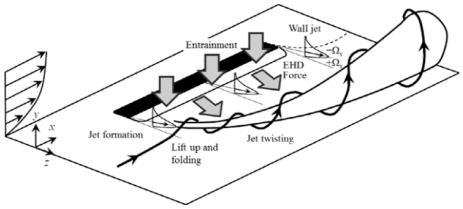

Fig. 4. Streamwise plasma actuator-induced vortex [30]

4 Experimental Setup

This study is divided into two experimental stages to demonstrate the capabilities of the DBD plasma actuator. The first stage focuses on developing a model to investigate constraints on electrode placement. With a 9V, 2A input to the boost-up power module, the effect of the actuator on vortex formation at the trailing edge is analyzed. The second stage involves simulating the NACA 23015 airfoil (maximum thickness 15% at 30% chord) in *ANSYS Fluent*. The lift coefficient (C_l) and drag coefficient (C_d) are compared under plasma actuator ON and OFF states to evaluate their impact on aerodynamic performance.

4.1 Plasma Actuator Model

i. Airfoil

The plasma actuator model was applied to the Clark-Y airfoil [31], a semi-symmetrical airfoil with a flat lower surface and a maximum thickness of 11.7% located approximately 30% of the chord length from the leading edge. Commonly used in general aviation and subsonic aircraft, the Clark-Y airfoil is valued for its predictable stall characteristics and ability to generate high lift at low angles of attack (AoA). As shown in Figure 5, the lift coefficient (C_l) for the Clark-Y airfoil (*see* Fig. 6) exhibits a linear increase with AoA, as plotted by *Airfoil Tools* [31], until a critical angle between 15°–18°. At this critical AoA, the airfoil reaches its maximum lift coefficient ($C_{l,max}$), after which the lift decreases sharply due to stall caused by airflow separation. The current paper selected a chord length of 110 mm to align with prior optimization research on airfoil designs to enhance aerodynamic performance and flow behavior [32-35]. This dimension ensures compatibility with the subsonic wind tunnel at the Aerospace Lab at Amity University Dubai [36], which has dimensions of 140 x 110 x 110 mm. This setup enables detailed observation of vortex formation at the trailing edge, contributing to a deeper understanding of flow dynamics and to improvements in aerodynamic efficiency.

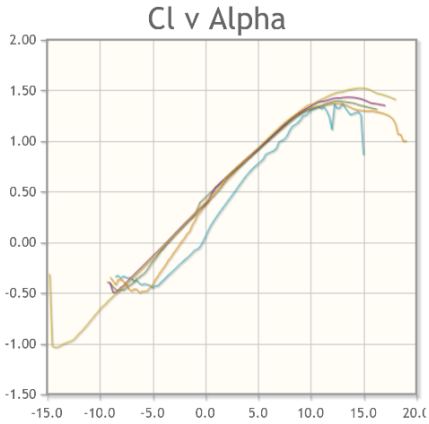

Fig. 5. Performance of C_l over AoA at Reynold number of 100 k [31]

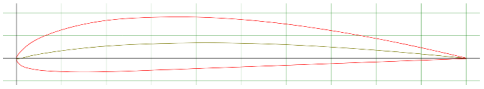

Fig. 6. Clark-Y airfoil [31]

ii. Structure

The model's structure was constructed using a foam board, selected for its exceptional versatility, lightweight properties, and cost-effectiveness, key factors in experimental aerodynamics. Foam board offers ease of molding, enabling precise shaping to replicate the desired airfoil geometry with high accuracy. Its smooth surface minimizes disturbances to the boundary-layer flow, ensuring reliable, consistent aerodynamic measurements during testing. Additionally, the material's lightweight nature reduces the overall mass of the setup, simplifying handling and facilitating secure mounting in experimental configurations such as subsonic wind tunnels. This combination of precision, efficiency, and practicality makes foam board an ideal choice for constructing models in plasma-based flow control studies.

iii. Electrodes

The electrodes were fabricated from thin 0.15 mm metal sheets, chosen for their excellent conductivity, lightweight properties, and flexibility, to facilitate seamless integration into the model. They were spaced 20 mm apart to maintain a uniform and stable electric field while minimizing the risk of electrical arcing that could interfere with consistent plasma formation. The electrode positioning was meticulously optimized for maximum ionization and effective airflow modification. This optimization ensured the plasma actuator operated efficiently, delivering the desired flow-control performance by enhancing boundary-layer interaction and minimizing energy losses. These design choices align with the operational requirements to maximize aerodynamic efficiency and maintain system reliability during testing.

iii. Dielectric Mediums

The dielectric medium was constructed using insulating tape, with two layers applied, each 0.14 mm thick, to ensure effective insulation of the electrodes. This dual-layer configuration was chosen to enhance the system's breakdown voltage, providing robust electrical insulation while maintaining the flexibility needed for smooth, precise application. The dielectric medium played a crucial role in sustaining stable plasma discharge by preventing electrical breakdown and ensuring consistent performance at high operating voltages. This design not only facilitated reliable operation but also optimized energy transfer to generate a steady ionic wind. The simple yet efficient setup offered an ideal solution for studying plasma-based flow control, combining stability, ease of assembly, and high performance to support detailed investigations into aerodynamic enhancements.

iv. Experimental Model

The construction and configuration of the experimental model, as illustrated in Figure 7, were meticulously designed to facilitate a comprehensive investigation into the effects of plasma on flow dynamics. The assembled model highlights the precise arrangement of the electrodes, the layered dielectric medium, and the integrated power system, ensuring optimal functionality and performance.

Fig. 7. Experimental Clark-Y airfoil

The Clark-Y airfoil cross-section was securely mounted to the subsonic wind tunnel adapter at a zero AoA, providing a controlled environment for studying plasma-induced flow modifications. Figure 7 also details the setup, showcasing the streamlined integration of the components, while Figure 8 presents the exact dimensions of the model. This thoughtful design enabled accurate observations and reliable data collection, contributing to a deeper understanding of plasma-based flow-control mechanisms.

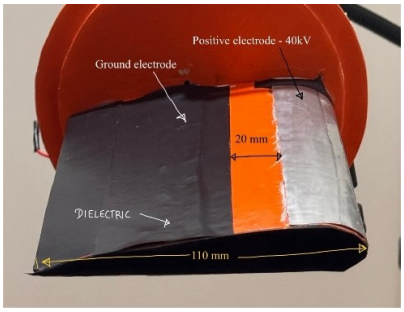

Fig. 8. Airfoil dimensions

v. High-Voltage Power Supply

The plasma actuator system was powered by a direct current (DC) boost-up power module (*see* Figure 9) capable of delivering up to 40 kV of high-voltage output. This module was specifically chosen for its ability to provide the necessary electric field strength to ionize air and generate plasma efficiently. Its design follows the schematic shown in Figure 10, ensuring a reliable and consistent high-voltage supply to the system. The high voltage is critical for establishing a stable plasma discharge, which drives the desired flow modifications. The module's output was connected to the actuator's electrodes, with one electrode serving as the high-voltage source and the other grounded. The electrode spacing and dielectric material properties were carefully optimized to prevent electrical arcing and maximize discharge stability. The electric field strength E, a key factor in generating the ionic wind, is directly influenced by the applied voltage V and the electrode spacing d, as described in Eq. 4:

$$V = E \cdot d \tag{4}$$

A stronger electric field enhances ionization and increases the intensity of the ionic wind, making the field strength a critical parameter in plasma-based flow control. This optimized setup ensures efficient plasma generation and effective manipulation of flow dynamics, contributing to the overall success of the experimental study. For the current model, with

V = 40 kV and d = 20mm, the most appropriate flow characteristic of the ion wind was observed between the electrodes, and no arcing occurred between them. Therefore, this model has an electric field of 2,000,000 V/mm (2kV/mm).

Fig. 9. Power Module with input (left) and output (right)

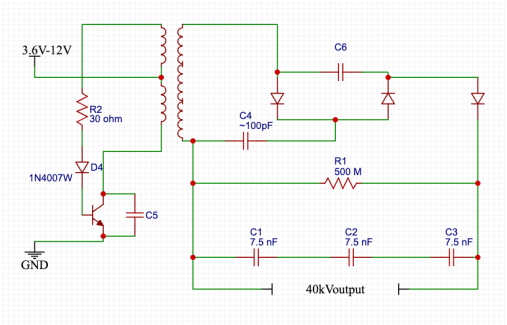

Fig. 10. The schematic design of the boost-up power module (created from EDA software)

2. Visual Confirmation

When the plasma actuator is energized, the plasma discharge is typically invisible to the human eye under normal lighting conditions due to its low luminosity. However, in a dark environment, the plasma becomes visible as a faint glow near the actuator's surface, which indicates the ionization of air molecules, a critical process for generating the ionic wind. The ionic wind is produced when charged particles accelerate in response to the electric field, creating a flow of ionized air. To observe this phenomenon, the test was conducted in a completely dark room with the camera set to ISO 12500, an aperture of f/1.78, and an exposure time of 3 seconds. Figure 11 illustrates the interaction between the flow and the surrounding air in this dark setting. This interaction generates a thin boundary layer with enhanced momentum near the actuator's surface, highlighting the plasma actuator's effectiveness in modifying airflow and controlling boundary-layer dynamics. The faint glow and the resulting airflow behavior provide valuable insights into the mechanism of ionic wind generation and its impact on aerodynamic performance.

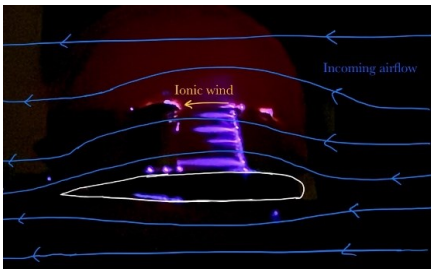

Fig. 11. Plasma actuator under dark conditions, showing the ion wind flow generated over the surface

3. Wind Tunnel Testing

A real-scale model test was conducted in the C15-10, a computer-controlled subsonic wind tunnel at the Aerospace Lab at Amity University Dubai. The test was performed at a flow velocity of 20 m/s and a static pressure of 33 mm. The first test was carried out with the plasma actuators in the OFF state. As expected, the results showed a significant pressure difference, leading to turbulent airflow at the trailing edge, as depicted in Figure 12 (left). The second test involved activating the plasma actuators (ON state), and the results demonstrated a noticeable improvement in flow characteristics at the trailing edge. The flow exhibited smooth, continuous dynamics, indicating a significant reduction in induced drag experienced by the airfoil, as shown in Figure 12 (right). These findings validate the study's objective of enhancing flow characteristics around the airfoil, confirming that the plasma actuators effectively improve aerodynamic performance by stabilizing airflow and reducing drag.

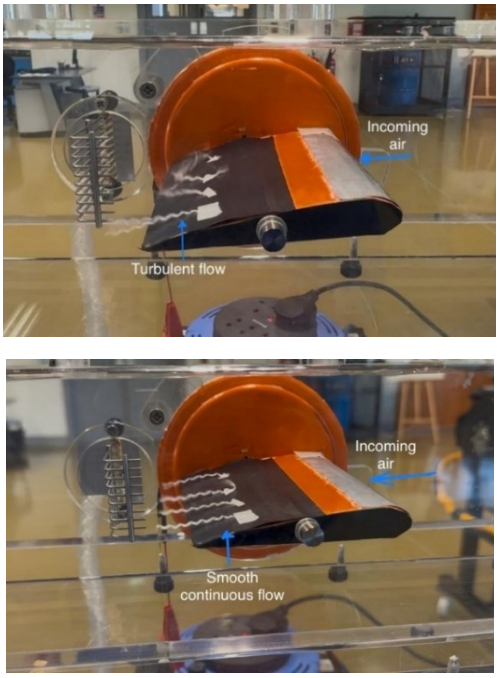

Fig. 12. Observation when the plasma state is OFF (first) and ON (second)

5 ANSYS FLUENT Model

This paper investigates flow separation control using plasma actuators on the NACA 23015 airfoil with a chord length of 1 m and a Reynolds number of 68,000. Computational fluid dynamics (CFD) simulations were used to evaluate the effectiveness of plasma actuators in controlling flow separation. It is crucial to note that the flow separation observed in this study is influenced by the Reynolds number, which plays a significant role in shaping the near-wall flow field [28]. The incoming airflow was set to 1 m/s, and the extracted values are presented in Table 1. The analysis reveals a noticeable increase in the lift coefficient (C_l) and a reduction in the drag coefficient (C_d), as illustrated in Figures 13 and 14 [20,21]. These results underscore the positive impact of plasma actuators on aerodynamic performance, enhancing lift and reducing drag by mitigating flow separation and stabilizing the boundary layer.

Table 1. C_d and C_l data on different attack angles

Alpha	Data			
	Simulation		Plasma=5	
	C_d	C_l	C_d	C_l
0	0.024	0.113	0.022	0.265
2	0.025	0.303	0.020	0.489
4	0.028	0.483	0.019	0.712
6	0.032	0.653	0.020	0.926
8	0.039	0.797	0.022	1.129
10	0.051	0.899	0.027	1.312

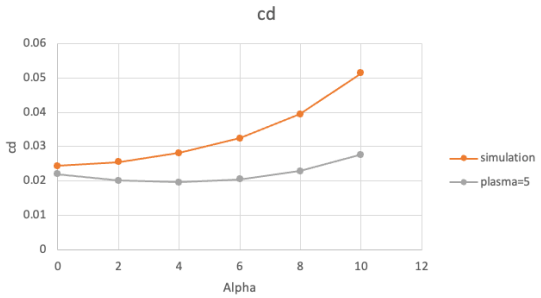

Fig. 13. Drag coefficient (C_d) vs Angle of Attack (alpha)

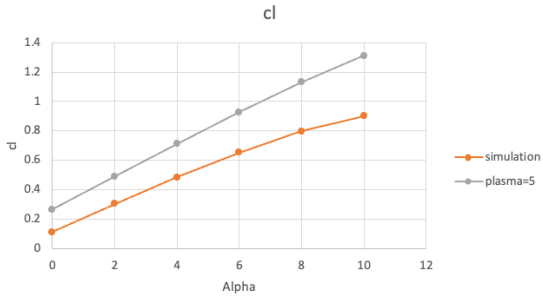

Fig. 14. Lift coefficient (C_l) vs Angle of Attack (alpha)

Figure 15 illustrates the velocity flow around the airfoil at zero angle of attack with the plasma actuator in the OFF state. In contrast, Figure 16 shows the flow representation when the actuator is ON. The results demonstrate smoother airflow over the surface and a noticeable reduction in flow separation. This improvement is directly attributed to the plasma actuator's ability to energize the boundary layer by introducing ionic wind, which imparts additional momentum to the near-wall flow. This enhanced interaction helps stabilize the flow, particularly in areas prone to separation, such as the leading edge and regions with adverse pressure gradients. The numerical simulations closely aligned with the experimental results, confirming the beneficial effects of plasma actuation on aerodynamic performance. A key finding from the simulations was that the lift coefficient (C_l) increased when the plasma actuator was activated. This improvement can be traced back to the actuator's role in suppressing flow separation, which is crucial for maintaining stable airflow over the airfoil. By delaying the onset of flow separation, the plasma actuator effectively reduced drag while enhancing the lift generated by the airfoil surface. Notably, a 40% increase in the lift coefficient was observed with the application of a magnitude five plasma actuator. However, it is essential to acknowledge that the scale of this system is minimal compared to commercial aviation, and the

impact of these results would likely differ significantly in larger-scale applications. Nonetheless, these findings provide valuable insights into the potential of plasma-based flow control for enhancing aerodynamic performance, especially in smaller-scale or experimental settings.

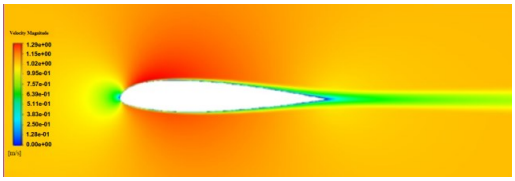

Fig. 15. Velocity Graph when the plasma actuators is OFF

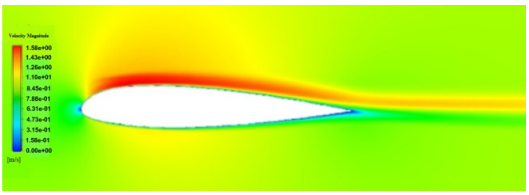

Fig. 16. Velocity Graph when the plasma actuators is ON

6 Discussion

The plasma actuator model profoundly impacted the boundary layer, significantly improving the system's aerodynamic performance. By reducing drag and stabilizing airflow, the actuator improved the model's overall aerodynamic efficiency. The simulations revealed that the plasma actuator helped maintain a more uniform velocity gradient within the boundary layer, minimizing velocity discrepancies and reducing turbulence. This improved flow stability was particularly important at higher angles of attack, where flow separation would typically occur more rapidly. However, the materials used for electrodes and dielectrics are prone to degradation under intense operating conditions, limiting their durability. Environmental factors such as humidity and pressure fluctuations further complicate the consistency of plasma discharge, adding to the technology's reliability challenges. Moreover, plasma actuator systems are expensive due to the specialized materials and high-voltage equipment required, making them less competitive compared to traditional aerodynamic control methods, such as mechanical surfaces or vortex generators. The technology also faces limitations due to limited long-term testing, leaving uncertainties about wear, reliability, and integration with existing systems. Significant redesigns would be necessary to accommodate plasma actuators within current aircraft systems, thereby increasing complexity and cost. Despite these challenges, the study of plasma-based flow control indicates promising applications for both commercial and military aerospace sectors. For commercial aviation, plasma actuators offer substantial benefits, particularly by improving fuel efficiency and stability during critical phases of flight, such as takeoff and landing. By enhancing lift and reducing drag, plasma actuators can optimize the lift-to-drag ratio, reduce fuel consumption, and enhance the economic performance of commercial aircraft, making them a potential game-changer for future aviation technologies.

7 Conclusion

Plasma-based flow control is promising to improve aerodynamic efficiency by modifying the boundary layer, delaying flow separation, and enhancing lift. Plasma actuators increase lift-to-drag ratios, improving fuel efficiency and stability during critical phases like takeoff, landing, and high-angle maneuvers. They benefit commercial aviation by reducing drag and improving low-speed stability, and military aviation by enhancing maneuverability and control at high speeds or AoA. In space exploration, plasma actuators can manage heat during atmospheric re-entry and improve aerodynamic stability at hypersonic speeds. Future research should focus on optimizing designs,

reducing power consumption, and testing scalable configurations for next-generation aerospace systems. Future research should focus on optimizing actuator designs, reducing power consumption, and developing scalable configurations for broader applications in the aerospace industry, including commercial, military, and space exploration vehicles. Future research should optimize actuator designs, reduce power consumption, explore novel electrode configurations, and enhance scalability for broader applications. Additionally, integrating plasma actuators with advanced control systems and testing their effectiveness in real-world flight scenarios will be critical to unlocking their full potential in next-generation aerospace systems.

Declaration of Competing Interest

The authors declare that they have no known competing financial interests or personal relationships that could have influenced the work reported in this paper.

Conflict of Interest Statement

There is no conflict of interest regarding the publication of this paper.

References

1. Moreau, E., Airflow control by non-thermal plasma actuators. *Journal of Physics D: Applied Physics*, 40(3), 605–636 (2007).
2. Thomas, F. O., Corke, T. C., & Patel, M., Plas,ma actuators for separation control on stationary and oscillating airfoils. *AIAA Journal*, 47(12), 2820–2831 (2009).
3. Enloe, C. L., McLaughlin, T. E., Van Dyken, R. D., et al., Mechanisms and responses of a single dielectric barrier plasma actuator: Plasma morphology. *AIAA Journal*, 42(3), 595–604 (2004).
4. Corke, T. C., Enloe, C. L., & Wilkinson, S. P. Dielectric barrier discharge plasma actuators for flow control. *Annual Review of Fluid Mechanics*, 42, 505–529 (2010).
5. Debien, A., Auffray, J., & Deleuze, A., Sliding discharge for plasma flow control: Electrical properties. *Journal of Electrostatics*, 70(2), 171–181 (2012).
6. Little, J., Nishihara, M., Adamovich, I., & Samimy, M., High-lift airfoil leading edge separation control using nanosecond pulse-driven DBD plasma actuators. *Experiments in Fluids*, 48(4), 521–537 (2010).
7. Pons, J., & Moreau, E., Corona discharge actuators for airflow control. *Journal of Electrostatics*, 66(7–8), 440–445 (2008).
8. Kimmel, S., & Ricker, R. Glow discharge plasma actuators for flow acceleration. *Plasma Science and Technology*, 13(2), 238–243 (2011).
9. Patel, M., Corke, T. C., & Gordeyev, S. Plasma flow control with peristaltic-like plasma actuators. *AIAA Paper*, 2007-1037 (2007).
10. Zong, H., & Kotsonis, M., Vectorized plasma actuators: A new approach for directional flow control. *AIAA Journal*, 53(10), 2858–2869 (2015).
11. Choi, K. S., Jukes, T. N., Whalley, R. D., Feng, L., Wang, J., Matsunuma, T., & Segawa, T., Plasma virtual actuators for flow control. *Journal of Flow Control, Measurement & Visualization*, *3*(01), 22 (2014).
12. Thomas, F., & Huang, J., *Documentation and Control of Flow Separation on a Low Pressure Turbine Linear Cascade of Pak-B Blades Using Plasma Actuators* (No. NASA/CR-2007-214677) (2007).
13. Grundmann, S., & Tropea, C., Experimental transition delay using glow-discharge plasma actuators. *Experiments in fluids*, *42*, 653-657 (2007).
14. Poggie, J., McLaughlin, T., & Leonov, S., Plasma aerodynamics: current status and future directions. *Aerospace Lab*, (10) (2015).
15. W. Strunk Jr., E.B. White, The Elements of Style, third ed., Macmillan, New York, 1979.
16. Asada, K., Ninomiya, Y., Fujii, K., & Oyama, A. (2009, January). Airfoil flow experiment on the duty cycle of DBD plasma actuator. In *47th AIAA Aerospace Sciences Meeting including The New Horizons Forum and Aerospace Exposition* (p. 531).
17. Benard, N., & Moreau, E., Electrical and mechanical characteristics of surface AC dielectric barrier discharge plasma actuators applied to airflow control. *Experiments in Fluids*, *55*, 1-43 (2014).
18. Neretti, G., Active flow control by using plasma actuators. *Recent Progress in Some Aircraft Technologies*, *1*, 13 (2016).
19. Cristofolini, A., Borghi, C. A., & Neretti, G., Charge distribution on the surface of a dielectric barrier discharge actuator for fluid-dynamic control. *Journal of Applied Physics*, *113*(14) (2013).
20. Borghi, C. A., Cristofolini, A., Grandi, G., Neretti, G., & Seri, P., A plasma aerodynamic actuator supplied by a multilevel generator operating with different voltage waveforms. *Plasma Sources Science and Technology*, *24*(4), 045018 (2015).
21. Borghi, C. A., Carraro, M. R., Cristofolini, A., & Neretti, G., Electrohydrodynamic interaction induced by a dielectric barrier discharge. *Journal of Applied Physics*, *103*(6) (2008).
22. Cristofolini, A., Neretti, G., Roveda, F., & Borghi, C. A., Schlieren imaging in a dielectric barrier discharge actuator for airflow control. *Journal of Applied Physics*, *111*(3) (2012).
23. Cristofolini, A., Neretti, G., & Borghi, C. A., Effect of the charge surface distribution on the flow field induced by a dielectric barrier discharge actuator. *Journal of Applied Physics*, *114*(7) (2013).
24. Neretti, G., Cristofolini, A., Borghi, C. A., Gurioli, A., & Pertile, R., Experimental results in DBD plasma actuators for airflow control. *IEEE Transactions on Plasma Science*, *40*(6), 1678-1687 (2012)
25. F.O. Thomas, T.C. Corke, M. Iqbal, A. Kozlov, and D. Schatzman. Optimization of Dielectric Barrier Discharge Plasma Actuators for Active Aerodynamic Flow Control. AIAA Journal. 2009;47:2169–2178. DOI: 10.2514/1.41588

26. Corke, T. C., Enloe, C. L., & Wilkinson, S. P., Dielectric barrier discharge plasma actuators for flow control. *Annual review of fluid mechanics*, *42*(1), 505-529 (2010).
27. Font, G. I., Enloe, C. L., & McLaughlin, T. E. Plasma volumetric effects on the force production of a plasma actuator. *AIAA journal*, *48*(9), 1869-1874 (2010).
28. West, T., & Hosder, S., Numerical investigation of plasma actuator configurations for flow separation control at multiple angles of attack. In *6th AIAA flow control conference* (p. 3053) (2012).
29. Neretti, G., Cristofolini, A., & Borghi, C. A., Experimental investigation on a vectorized aerodynamic dielectric barrier discharge plasma actuator array. *Journal of Applied Physics*, *115*(16) (2014).
30. Choi, K. S., Jukes, T. N., Whalley, R. D., Feng, L., Wang, J., Matsunuma, T., & Segawa, T., Plasma virtual actuators for flow control. *Journal of Flow Control, Measurement & Visualization*, *3*(01), 22 (2014).
31. Ntantis EL, Xezonakis V. Aerodynamic design optimization of a NACA 0012 airfoil: An introductory adjoint discrete tool for educational purposes. *International Journal of Mechanical Engineering Education*. 53(3):611-630 (2024).
32. Airfoil Tools (2024, November 3). *Clark Y Airfoil (clarky-il)*. http://airfoiltools.com/airfoil/details?airfoil=clarky-il#polar
33. Ntantis, E.L., Francis, E., Pugazendi, V., George, J., Tarek, A., Emthias, M., & Rasheed, S., Study of sinusoidal perturbations on the leading edge of an aircraft wing. Journal of Aeronautics, Astronautics, and Aviation, 53(3), 375-386 (2021).
34. Ntantis, E.L., & Xezonakis, V., Improving transonic performance with adjoint-based NACA 0012 airfoil design optimization. Results in Engineering, 24, 103189 (2024).
35. Ntantis, E.L., Francis, E., Fazel, H., George, J., Blal, M., Emthias, M., & Pugazendi, V., Numerical study on a supersonic flow around a bullet. WSEAS Transactions on Fluid Mechanics, 18, 1-9. 12 (2023).
36. David, L.C.F., Pazo, J., Ntantis, E.L., Siddharth, K.S. Cross-Correlation of Schlieren Images to Retrieve Velocity Information. In: Sharma, R., Kannojiya, R., Garg, N., Gautam, S.S. (eds) Advances in Engineering Design. FLAME 2022. Lecture Notes in Mechanical Engineering. Springer, Singapore (2023).
37. Patel, M. P., Ng, T. T., Vasudevan, S., Corke, T. C., & He, C., Plasma actuators for hingeless aerodynamic control of an unmanned air vehicle. *Journal of Aircraft*, *44*(4), 1264-1274 (2027).